Highly Stabilized Low-Spin Iron(III) and Cobalt(III) Complexes of a Tridentate Bis-Amide Ligand 2,6-Bis(*N*-phenylcarbamoyl)pyridine. Novel Nonmacrocyclic Tetraamido-N Coordination and Two Unusually Short Metal−Pyridine Bonds

Manabendra Ray, Debalina Ghosh, Zahida Shirin, and Rabindranath Mukherjee*

Department of Chemistry, Indian Institute of Technology, Kanpur 208 016, India

Received September 11, 1996

Introduction

Investigations of the coordination chemistry of iron(III)[1−3] and cobalt(III)[4−7] with nonmacrocyclic chelating ligands containing an amide functionality have received much attention in recent years. These studies have revealed that the deprotonated nitrogens of organic amides, being anionic in nature, are capable of stabilizing the trivalent oxidation state to a considerable extent; hence the prospect of facile entry into higher oxidation states of these metal ions.[3,6] It is worth noting here that only a handful of stable low-spin iron(III) complexes of this class have been prepared[1b−d,2] and some have been structurally characterized.[1b,d,2a,b]

In order to develop further the coordination chemistry of pyridine amide ligands toward iron and cobalt ions, new ligands must be exploited. As a first step toward this goal we have initiated a program to explore the coordination chemistry of a simple, easily synthesizable, tridentate dianioic bis-amide ligand L(2−) [H_2L = 2,6-bis(*N*-phenylcarbamoyl)pyridine]. Here we describe the synthesis, X-ray structures, and spectral, magnetic, and redox properties of two novel six-coordinate low-spin iron(III) and cobalt(III) complexes, $[Et_4N][FeL_2]\cdot 1.5H_2O$ (**1**) and $[Et_4N][CoL_2]\cdot 2H_2O$ (**2**).

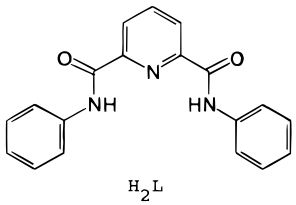

H_2L

Experimental Section

Materials and Reagents. All chemicals were obtained from commercial sources and used as received. Solvents were dried as reported previously.[8] $Fe(MeCN)_4(ClO_4)_2$ and tetra-*n*-butylammonium perchlorate (TBAP) were prepared as before.[1c,8a]

Ligand Synthesis. 2,6-Bis(*N*-phenylcarbamoyl)pyridine (H_2L). The ligand has already been reported in the literature.[9a] Our synthetic methodology, which has been adapted from Barnes et al,[9b] is described below.

2,6-Pyridinedicarboxalic acid (3.0 g, 0.018 mol) was suspended in pyridine (10 mL), aniline (3.5 g, 0.038 mol) was added to the mixture, and the mixture was stirred for 10 min at ∼40 °C. Initially a white precipitate formed, which finally formed an emulsion. To this was added triphenyl phosphite (9.5 mL, 0.036 mol) dropwise, the temperature of the reaction mixture was increased to 90−100 °C, and the mixture was magnetically stirred for 4 h. After 12 h, it was washed with water and a white oil was obtained. Addition of methanol (20 mL) afforded white needles. This material was filtered off, washed with methanol, and dried in vacuo. Yield: 5.5 g (96%). ^{1}H NMR [d_6-dimethyl sulfoxide (DMSO)]: δ 8.41 (3H, m, pyridine ring protons); 7.96 (4H, 2H, J = 7.5 Hz), 7.56−7.11 (6H, m, phenyl ring protons).[9a]

Synthesis of Metal Complexes. (a) $[Et_4N][FeL_2]\cdot 1.5H_2O$ (1). The ligand H_2L (200 mg, 0.63 mmol) was dissolved in dinitrogen-flushed *N*,*N*′ -dimethylformamide (DMF) (10 mL), and to it was added solid NaH (30 mg, 1.25 mmol), resulting in a light yellow solution. $Fe(MeCN)_4(ClO_4)_2$ (132 mg, 0.315 mmol) was dissolved in DMF (5 mL) separately. The latter solution was then added to the ligand solution using a cannula under a dinitrogen atmosphere. The resulting solution was magnetically stirred for 2 h at 298 K. Exposure to air resulted in a color change from dark blue to orangish red. To this was added solid $[Et_4N]Cl\cdot xH_2O$ (104 mg, 0.63 mmol), and stirring was continued for 12 h. Removal of the solvent was followed by addition of MeCN (10 mL) and filtration. 0n concentration (∼4 mL) and addition of diethyl ether (∼8 mL) a dark reddish brown precipitate resulted (160 mg; ∼60%). Recrystallization from MeCN−Et_2O (vapor diffusion) afforded crystalline solid suitable for structural studies.

Characterization. Anal. Calcd for $C_{46}H_{49}N_7O_{5.5}Fe$: C, 65.48; H, 5.81; N, 11.63. Found: C, 66.12; H, 5.85; N, 11.72. Conductivity (MeCN, 10^{-3} M solution at 298 K): Λ_M = 150 Ω cm^2 mol^{-1}. Absorption spectra [λ_{max}, nm (ϵ, M^{-1} cm^{-1})]: (in MeCN) 254 (26 120), 300 sh (15 300), 440 (6220); (in DMF)

(1) Pyridine amide ligand: (a) Yang, Y.; Diederich, F.; Valentine, J. S. *J. Am. Chem. Soc.* **1991**, *113*, 7195. (b) Che, C.-M.; Leung, W.-H.; Li, C.-K.; Cheng, H.-Y.; Peng, S.-M. *Inorg. Chim. Acta* **1992**, *196*, 43. (c) Ray, M.; Mukherjee, R. N.; Richardson, J. F.; Buchanan, R. M. *J. Chem. Soc., Dalton Trans.* **1993**, 2451. (d) Wocadlo, S.; Massa, W.; Folgado, J.-V. *Inorg. Chim. Acta* **1993**, *207*, 199.

(2) Synthetic models of iron-bleomycins (metallo-bleomycins have among other ligands deprotonated amide nitrogen): (a) Tao, X.; Stephan, D. W.; Mascharak, P. K. *Inorg. Chem.* **1987**, *26*, 754. (b) Brown, S. J.; Olmstead, M. M.; Mascharak, P. K. *Inorg. Chem.* **1990**, *29*, 3229. (c) Guajardo, R. J.; Hudson, S. E.; Brown, S. J.; Mascharak, P. K. *J. Am. Chem. Soc.* **1993**, *115*, 7971. (d) Guajardo, R. J.; Tan, J. D.; Mascharak, P. K. *Inorg. Chem.* **1994**, *33*, 2838. (e) Guajardo, R. J.; Mascharak, P. K. *Inorg. Chem.* **1995**, *34*, 802.

(3) Salicylamide ligand: Koikawa, M.; Ōkawa, H.; Maeda, Y.; Kida, S. *Inorg. Chim. Acta* **1992**, *194*, 75.

(4) Pyridine amide ligand: (a) Saussine, L.; Brazi, E.; Robine, A.; Mimoun, H.; Fischer, J.; Weiss, R. *J. Am. Chem. Soc.* **1985**, *107*, 3534. (b) Mak, S.-T.; Wong, W.-T.; Yam, V. W.-W.; Lai, T.-F.; Che, C.-M. *J. Chem. Soc., Dalton Trans.* **1991**, 1915. (c) Ray, M.; Mukherjee, R. N. *Polyhedron* **1992**, *11*, 2625.

(5) Synthetic models of cobalt-bleomycins: (a) Delany, K.; Arora, S. K.; Mascharak, P. K. *Inorg. Chem.* **1988,** *27*, 705. (b) Muetterties, M.; Mascharak, P. K.; Cox, M. B.; Arora, S. K. *Inorg. Chim. Acta* **1989**, *160*, 123. (c) Brown, S. J.; Olmstead, M. M.; Mascharak, P. K. *Inorg. Chem.* **1989,** *28*, 3720. (d) Tan, J. D.; Hudson, S. E.; Brown, S. J.; Olmstead, M. M.; Mascharak, P. K. *J. Am. Chem. Soc.* **1992**, *114*, 3841. (e) Farinas, E.; Baidya, N.; Mascharak, P. K. *Inorg. Chem.* **1994**, *33*, 5970.

(6) Salicylamide ligand: (a) Anson, F. C.; Collins, T. J.; Coots, R. J.; Gipson, S. L.; Richmond, T. G. *J. Am. Chem. Soc.* **1984**, *106*, 5037. (b) Koikawa, M.; Gotoh, M.; Ōkawa, H.; Kida, S.; Kohzuma, T. *J. Chem. Soc., Dalton Trans.* **1989**, 1613.

(7) Alkoxide amide ligand: (a) Collins, T. J.; Richmond, T. G.; Santarsiero, B. D.; Treco, B. G. R. T. *J. Am. Chem. Soc.* **1986**, *108*, 2088. (b) Brewer, J. C.; Collins, T. J.; Smith, M. R.; Santarsiero, B. D. *J. Am. Chem. Soc.* **1988**, *110*, 423.

(8) (a) Ray, M.; Mukerjee, S.; Mukherjee, R. N. *J. Chem. Soc., Dalton Trans.* **1990**, 3635. (b) Gupta, N.; Mukerjee, S.; Mahapatra, S.; Ray, M.; Mukherjee, R. N. *Inorg. Chem.* **1992**, *31*, 139. (c) Ray, M.; Mukherjee, R. N.; Richardson, J. F.; Mashuta, M. S.; Buchanan, R. M. *J. Chem. Soc., Dalton Trans.* **1994**, 965.

(9) (a) Horino, H.; Sakaba, H.; Arai, M. *Synthesis* **1989**, 715. (b) Barnes, D. J.; Chapman, R. L.; Vagg, R. S.; Watton, E. C. *J. Chem. Eng. Data* **1978**, *23*, 349.

S0020-1669(96)01118-4 CCC: $14.00

302 (16 220), 337 sh (11 630), 441 (6850); (in DMSO) 302 (19 950), 441 (8925); (in H_2O) 248 (25 930), 305 sh (15 380), 422 (7110), 525 sh (1900).

(b) $[Et_4N][CoL_2]\cdot 2H_2O$ (2). To a solution of $Co(MeCO_2)_2\cdot 4H_2O$ (85 mg, 0.34 mmol) in DMF (10 mL) under a dinitrogen atmosphere was added $[Et_4N][MeCO_2]\cdot 4H_2O$ (88 mg, 0.34 mmol), generating blue-violet solution. The ligand H_2L (0.215 g, 0.68 mmol) was dissolved separately in DMF (10 mL) under a dinitrogen atmosphere, NaH (33 mg, 1.38 mmol) was added to the mixture, and the mixture was stirred for 30 min, generating a light yellow solution. The two solutions were then mixed, and a color change from an initial orange to yellowish brown with a greenish tinge was observed. On exposure to air the solution color darkened. After being stirred for 4 h, the reaction mixture was filtered and solvent removed in vacuo. To the solid thus obtained was added MeCN (10 mL), and the solution was filtered. Slow evaporation of this solution in air resulted in the formation of dark green crystals contaminated with some white impurity. Recrystallization was achieved by diethyl ether diffusion into an MeCN solution of the complex. Large dark green crystals were formed, which were washed with a 1:3 mixture of MeCN−Et_2O (v/v) and finally vacuum dried (yield: 160 mg, ∼55%).

Characterization. Anal. Calcd for $C_{46}H_{50}N_7O_6Co$: C, 64.56; H, 5.85; N, 11.46). Found: C, 64.60; H, 5.90; N, 11.50. Conductivity (MeCN, 10^{-3} M solution at 298 K): $\Lambda_M = 120$ $\Omega^{-1}cm^2\ mol^{-1}$. Absorption spectrum [$\lambda_{max}$, nm ($\epsilon$, $M^{-1}\ cm^{-1}$)]: (in MeCN) 254 (29 640), 299 (19 430), 335 sh (15 850), 455 sh (2100), 633 (90).

Physical Measurements. Solution electrical conductivity measurements were carried out with an Elico (Hyderabad, India) Type CM-82 T conductivity bridge. Spectroscopic data were obtained by using the following instruments: infrared spectra, Perkin-Elmer M-1320; electronic spectra, Perkin-Elmer Lambda 2; X-band EPR spectra, Varian E-109 C; ^1H NMR spectra, PMX-60 JEOL (60 MHz) and Brüker WP-80 (80 MHz) NMR spectrometer.

Variable-temperature (34−300 K) solid-state magnetic susceptibility measurements were done by the Faraday technique using a locally-built magnetometer. The setup consists of an electromagnet with constant gradient pole caps (Polytronic Corporation, Bombay, India), Sartorius M25-D/S balance (Germany), a closed-cycle refrigerator, and a Lake Shore temperature controller (Cryo Industries, USA). The system was calibrated with $HgCo(SCN)_4$.[10] The temperature-independent magnetic moment of $Fe(acac)_3$[10] was used to calibrate the temperature controller at low temperatures. All measurements were made at a fixed main field strength of ∼10 kG. The sample holder used in the experiments was measured at the same temperature points and field, and its moment was subtracted from the observed moment with sample present in order to obtain the moment due to the sample alone. The measurements were started at room temperature, and the sample was cooled and held at the desired temperature during the measurement. Each data point was the mean of three measurements. Solution-state magnetic susceptibility was obtained by the NMR technique of Evans[11] in MeCN with a PMX-60 JEOL (60 MHz) NMR spectrometer. Susceptibilities were corrected for the diamagnetic contribution, which was calculated to be -462×10^{-6} $cm^3\ mol^{-1}$ by using literature values.[10b]

Cyclic voltammograms were recorded on PAR equipment consisting of a model 174A polarographic analyzer with a model 175 universal programmer. A PAR model G0021 glassy carbon electrode was used as the working electrode. All potentials were referenced to the saturated calomel electrode (SCE). The values of $E_{1/2}$ were taken as $0.5(E_{pc} + E_{pa})$ where E_{pc} and E_{pa} are the cathodic and anodic peak potentials, respectively. Coulometry was performed by using a PAR model 377A cell system and a PAR model 173 potentiostat/galvanostat. A platinum wire−gauze electrode was used as working electrode. Further details of electrochemical measurements are already reported in the literature.[8a,b]

Crystal Structure Determinations. A deep red needle-shaped crystal of $[Et_4N][FeL_2]\cdot 1.5H_2O$ (**1**) (dimensions: $0.2 \times 0.2 \times 0.1$ mm) and a deep green well-formed crystal of $[Et_4N][CoL_2]\cdot 2H_2O$ (**2**) (dimensions: $0.4 \times 0.4 \times 0.3$ mm) were used for data collection. Diffracted intensities were collected on an Enraf Nonius CAD4-Mach diffractometer using graphite-monochromated Mo Kα radiation ($\lambda = 0.710\ 73$ Å). Lattice parameters for both complexes were obtained from least-squares analyses of 25 machine-centered reflections. Three standard reflections were measured at every hour to monitor instrument and crystal stability. Intensity data were corrected for Lorentz and polarization effects; analytical absorption corrections were applied. The XTAL3.2 program package[12] was used in absorption and all subsequent calculations, utilizing a PC-486 computer under MS-DOS version 5. The linear absorption coefficients, neutral atom scattering factors for the atoms, and anomalous dispersion corrections for non-hydrogen atoms were taken from ref 13. The structures were solved by the direct method and successive difference Fourier syntheses. The function minimized during full-matrix least-squares refinement was $\Sigma w(F_o - F_c)^2$ where $w^{-1} = 1/\sigma(F)$. The positions of the hydrogen atoms were calculated assuming ideal geometries of the atoms concerned, and their positions and thermal parameters were not refined. All other atoms were refined with anisotropic thermal parameters. For both of the complexes some disorder was observed with the Et_4N^+ cations. Two positions were identified as possible methylene carbon atoms, and they were refined with a site occupation factor of 0.5. The terminal methyl carbon sites C(24) showed large displacement parameters indicating some degree of disorder, but could not be resolved. Crystal data and a summary of experimental results are presented in Table 1. Selected bond distances and angles associated with the anionic parts are listed in Table 2. The rest of the crystallographic data have been submitted as Supporting Information.

Results and Discussion

Synthesis. The ligand H_2L was prepared by treating 2,6-pyridinedicarboxylic acid with aniline in the presence of triphenylphosphite in pyridine. The synthesis of **1** involved initial anaerobic reaction of Na_2L with $Fe(MeCN)_4(ClO_4)_2$ in DMF at 298 K to form a blue Fe(II) complex, which on air oxidation generates an orangish red Fe(III) complex. Addition of $[Et_4N]Cl\cdot xH_2O$ and the usual workup afforded dark reddish brown air-stable crystals of **1**. In the case of **2**, reaction of $Co(O_2CMe)_2\cdot 4H_2O$ and Na_2L in MeCN generates a yellowish brown cobalt(II) complex which on exposure to air and in the presence of $[Et_4N][MeCO_2]\cdot 4H_2O$ finally affords dark green crystals. For both complexes the absence of ν(N−H) in the IR spectrum confirms that the ligand is coordinated in the depro-

(10) (a) Figgis, B. N.; Lewis, J. *Prog. Inorg. Chem.* **1964**, *6*, 37. (b) O'Connor, C. J. *Prog. Inorg. Chem.* **1982**, *29*, 203.
(11) Evans, D. F. *J. Chem. Soc.* **1959**, 2003.
(12) Hall, S. R.; Flack, H. D.; Stewart, J. M., Eds. *The XTAL 3.2 Reference Manual*; Universities of Western Australia, Geneva, and Maryland, 1992.
(13) *International Tables for X-ray Crystallography*; Kynoch Press: Birmingham, England, 1974; Vol. IV.

Table 1. Crystal Data for $[Et_4N][FeL_2]\cdot 1.5H_2O$ (**1**) and $[Et_4N][CoL_2].2H_2O$ (**2**)

	1	**2**
empirical formula	$C_{46}H_{49}N_7O_{5.5}Fe$	$C_{46}H_{50}N_7O_6Co$
fw	843	855
temp, °C	20	20
radiation (λ, Å)	Mo Kα (0.710 73)	Mo Kα (0.710 73)
cryst syst	monoclinic	monoclinic
space group	C2/c (No. 15)	*C*2/c (No. 15)
a, Å	9.897 (4)	10.033(1)
b, Å	22.414 (5)	22.317 (7)
c, Å	19.693 (3)	19.641 (4)
β, deg	102.85 (2)	102.60 (1)
V, Å^3	4259.2 (2)	4291.7 (5)
Z	4	4
F(000), electrons	1776	1800
ρ(calcd), g cm^{-3}	1.316	1.324
μ (Mo Kα), mm^{-1}	0.41	0.46
min/max transm coeff	0.9066/0.9068	0.7883/0.7892
no. of unique reflcns	3321	2800
no. of reflcns used ($I > 3\sigma(I)$)	2529	1863
no. of variables	296	296
R^a	0.049	0.045
$R_w{}^b$	0.059	0.046
goodness of fit	2.062	1.874

^{a} $R = \Sigma(F_o - F_c)/\Sigma F_o$. ^{b} $R_w = [\Sigma w(F_o - F_c)^2/\Sigma w F_o^2]^{1/2}$, $w = 1/\sigma(F)$.

Table 2. Selected Bond Lengths (Å) and Angles (deg) in the Anioinic Parts of $[Et_4N][FeL_2]\cdot 1.5H_2O$ (**1**) and $[Et_4N][CoL_2]\cdot 2H_2O$ (**2**)

1		**2**	
Fe−N(1)	1.972 (3)	Co−N(1)	1.968 (4)
Fe−N(2)	1.874 (3)	Co−N(2)	1.845 (3)
Fe−N(3)	1.970 (3)	Co−N(3)	1.962 (4)
N(1)−Fe−N(2)	101.7 (1)	N(1)−Co−N(2)	100.5 (2)
N(1)−Fe−N(2′)	81.2 (1)	N(1)−Co−N(2′)	81.6 (2)
N(1)−Fe−N(3)	161.6 (1)	N(1)−Co−N(3)	162.6 (2)
N(1)−Fe−N(3′)	92.6 (1)	N(1)−Co−N(3′)	92.5 (2)
N(2)−Fe−N(3)	96.7 (1)	N(2)−Co−N(3)	96.8 (1)
N(2)−Fe−N(3′)	80.5 (1)	N(2)−Co−N(3′)	81.1(2)
N(1)−Fe−N(1′)	89.8 (1)	N(1)−Co−N(1′)	89.4 (2)
N(2)−Fe−N(2′)	176.1 (1)	N(2)−Co−N(2′)	177.1 (2)
N(3)−Fe−N(3′)	90.8 (1)	N(3)−Co−N(3′)	90.7 (2)

tonated form. The ν(OH) absorption is observed at ∼3600 cm^{-1}. Elemental analyses, IR, and solution electrical conductivity data (1:1 electrolyte)[14] are in agreement with the above formulations. Interestingly, **1** and **2** are soluble in MeCN, DMF, DMSO, and also in water.

Description of the Structures. Complexes **1** and **2** are isomorphous. Views of their anions are presented in Figures 1 and S1 (Supporting Information), respectively. As shown in Figure 1, the Fe atom sits on an imposed C_2 axis and is coordinated by four deprotonated amide nitrogens in the equatorial plane [N(1) and N(3) and their symmetry related] and two pyridyl nitrogens [N(2) and its symmetry related] in the axial positions. The dihedral angle between the coordinating planes N(1)−M−N(2) and N(2)−M−N(3) is 178.69(4)° for **1** and 178.82(7)° for **2**, revealing meridional coordination of L(2−).

The geometry of the MN_6 coordination polyhedra is appreciably compressed octahedral (Table 2). Significant deviation from 90° of the bond angles involving the chelation is observed (Table 2) presumably due to formation of five-membered chelate rings with extended conjugation. Further evidence of strain in the chelate rings arises from the following observation. For both structures, although in each ligand the two *N*-phenyl rings and the pyridine ring are planar, the two phenyl rings, however, make an angle of ∼81° (**1**) and ∼79° (**2**) to each other and they make angles of ∼94° and ∼118° for **1** and ∼96°and ∼117° for **2**, with the central pyridine ring.

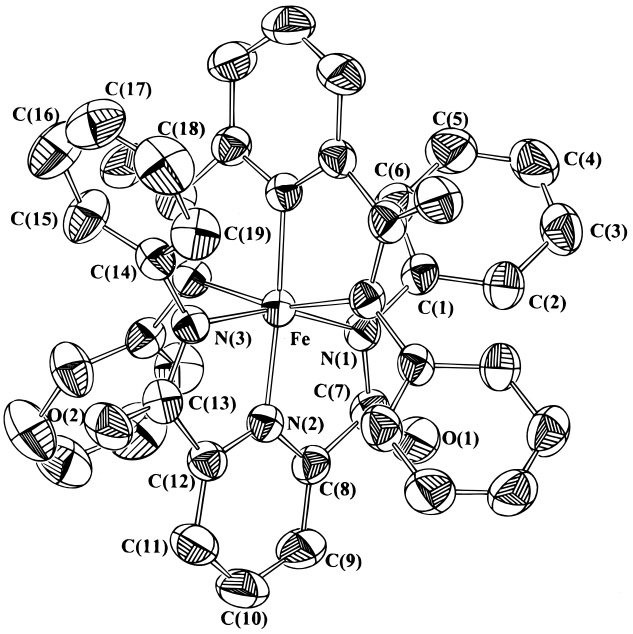

Figure 1. View of the structure of the anion $[FeL_2]^-$ in the crystal of its tetraethylammonium salt, $[Et_4N][FeL_2]\cdot 1.5H_2O$ (**1**). Hydrogen atoms are omitted for clarity. Unlabeled atoms are related to labeled atoms by the crystallographic 2-fold axis.

The average $M-N_{amide}$ bond lengths are sligthly on the longer side compared to those of reported complexes with amide ligands.[1b,d,2a,b,5a,b,d] A very interesting feature of these two structures is the $M-N_{py}$ bond length, which is significantly shorter (∼0.1 Å) than that observed for related structures.[1b,d,2a,5a,15] In fact, within the family of $M^{III}N_6$ ($S = 1/2$ for Fe and $S = 0$ for Co) complexes with peptide ligands **1** and **2** exhibit the shortest $Fe-N_{py}$ and longest $Fe-N_{amide}$ bond distances. Due to the strong donor capacity of deprotonated amide N donors providing four negative charges on the equatorial plane, it is expected to have shorter $M-N_{amide}$ bond lengths. We are inclined to believe that the observed longer $M-N_{amide}$ bonds and shorter $M-N_{pyridine}$ bonds are the result of steric predominance over electronic effects.

Absorption Spectra. In MeCN, DMF, and DMSO solution **1** exhibits an intense ligand-to-metal charge transfer (LMCT) band at ∼440 nm (Figure S2, Supporting Information). In water this band is at ∼420 nm with an additional shoulder at 520 nm. In MeCN solution **2** exhibits a single ligand field transition at 633 nm. Considering pseudo-octahedral symmetry we assign this to the $^1A_1 \rightarrow {}^1T_1$ origin.[16] It is quite possible that the expected $^1A_1 \rightarrow {}^1T_2$ transition is hidden under the charge-transfer band ∼460 nm (Figure S2).

EPR Spectra and Magnetism of 1. We have investigated the EPR spectral behavior of **1** in the solid state as well as in solution at 298 K (Figures S3 and S4, Supporting Information). While in MeCN solution it exhibits an isotropic signal at $g = 2.115$; in the polycrystalline state and in water−ethylene glycol mixture (1:2 v/v) it displays an axial spectrum [*g* values: 2.190 and 1.940 (solid); 2.160 and 1.990 (solution)], characteristic of

(14) Geary, W. J. *Coord. Chem. Rev.* **1971**, *7*, 81.

(15) (a) Arulsamy, N.; Hodgson, D. J. *Inorg. Chem.* **1994**, *33*, 4531. (b) Bernhardt, P. V.; Comba, P.; Mahu-Rickenbach, A.; Steblere, S.; Steiner, S.; Varnagy, K.; Zehnder, M. *Inorg. Chem.* **1992**, *31*, 4194.

(16) Cotton, F. A.; Wilkinson, G. *Advanced Inorganic Chemistry*, 5th ed.; Wiley: New York, 1988; pp 721, 734.

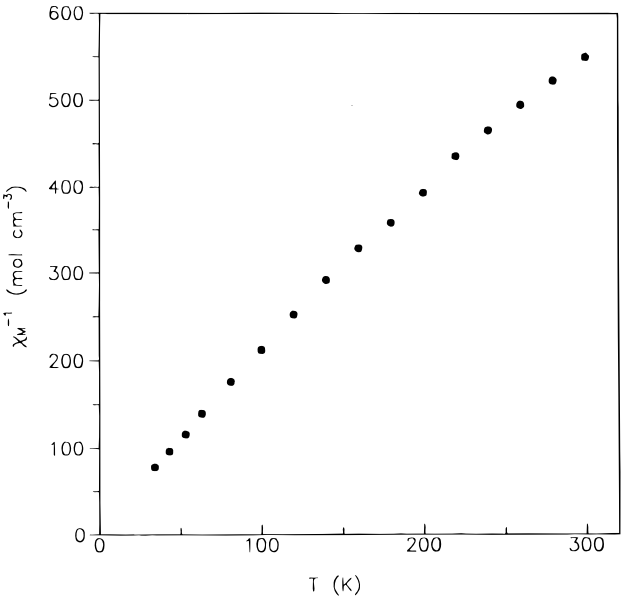

Figure 2. Plot of reciprocal molar susceptibility vs temperature for $[Et_4N][FeL_2]\cdot 1.5H_2O$ (**1**).

a low-spin iron(III) complex, with large deviation from octahedral symmetry.[17]

The effective magnetic moment of **1** in MeCN solution is 2.38 μ_B (300 K), corresponding to an $S = {}^1/_2$ state with an appreciable orbital contribution.[18] In order to investigate, in detail, its solid state magnetic behavior, variable-temperature (34−300 K) measurements were performed (Figure 2). The moment of 2.09 μ_B at 300 K is appreciably lower than that in MeCN solution. The solid state result is in conformity with EPR and structural results, revealing appreciable axial distortion. The increased moment in MeCN solution could be due to a relaxed (more toward octahedral) coordination sphere. As the temperature is lowered, the moment decreases toward the spin only value, as expected (μ_{eff} at 81 K is 1.92 μ_B).[16]

^{1}H NMR Spectrum of 2. Comparing the ^{1}H NMR spectra of the protonated ligand H_2L (in d_6-DMSO) (Figure S5, Supporting Information) and diamagnetic complex **2** in (CD_3-CN) (Figure S6, Supporting Information), we observe that all free ligand proton chemical shifts move upfield, i.e., negative coordination-induced shifts ($\Delta\delta = \delta_{complex} - \delta_{ligand}$),[19] upon coordination. For phenyl ring protons this could arise if all lie over the shielding plane of the central pyridine ring of the other coordinated ligand. The effect upon the pyridine hydrogens could be due to $Co^{III} \rightarrow \pi^*$ donation. Thus we observe that the solid-state structure is retained in solution.

Redox Properties. To investigate the extent of stabilization of the metal (III) state toward reduction and to examine whether or not oxidative responses corresponding to the accessibility of higher oxidation states could be achieved, cyclic voltammetric studies were performed.

(a) The M(III)−M(II) Redox Process. Cyclic voltammograms of **1** (Figure S7, Supporting Information) and **2** (Figure S8, Supporting Information) in MeCN solution at a glassy carbon electrode show a one-electron M(III)−M(II) reductive[20] response with $E_{1/2}$ values of −0.91 V (**1**) and −1.10 V (**2**) vs SCE. While for **1** the response is quasireversible ($\Delta E_p = 80$ mV),[8b] for **2** occurrence of a structural change due to reduction ($\Delta E_p = 240$ mV) is implied. This is understandable given the fact that deprotonated amide nitrogens are not good donors for cobalt(II).[21]

Compared to similar complexes[1b,c,2a,b,4b,5a,b] with amide ligands the M(III) state is highly stabilized in **1** and **2**. In fact, the observed potentials are the lowest. This effect must be due to the presence of four deprotonated amide nitrogen coordination, which stabilizes the metal(III) state to a considerable extent. The stereochemical requirement of the ligand framework could also contribute to this effect. Another factor which can contribute is the difference in overall charge of **1** and **2** to that of the related complexes.

(b) Solvent Dependency of the Fe(III)−Fe(II) Redox Process. Due to its ready solubility in many solvents we investigated the redox behavior of **1** as a function of solvent: MeCN, DMF, DMSO, and water. It is worth noting that in going from MeCN to water the $E_{1/2}$ value shifts anodically by 400 mV. This investigation reveals that the Fe(II) state of the complex $[FeL_2]^{2-}$ is systematically better stabilized due to enhanced solvation, as the dielectric constant of the medium is increased. Interestingly, the Fe(III)−Fe(II) reduction potentials correlate linearly with the inverse of the dielectric constant of the medium (Figure S9, Supporting Information), in line with the free energy of solvation as predicted by the Born equation.[22a,b] As the solvent coordination[22c] is not expected in **1**, the redox potentials do not follow any trend when plotted against the Gutmann donor number.[22b]

(c) Ligand Oxidation. In MeCN solution **1** and **2** display an additional oxidative response at 1.05 V (**1**) and 1.17 V vs SCE (Figures S7 and S8, respectively). Chemically (Ce^{4+}) as well as coulometrically generated 1e$^-$-oxidized species of **1** in MeCN are stable for at least 1 h, under dry anaerobic conditions.[23] The greenish brown solution thus obtained displays an absorption band at ∼670 nm. Similar spectral behavior was observed with pyridine amide systems showing ligand-centered oxidation.[1b,c,4b,c]

Summary. The following are the principal findings and conclusions of this investigation.

(1) To the best of our knowledge, this report documents the first example of synthesis and X-ray strutural characterization of trivalent iron and cobalt complexes having nonmacrocyclic tetraamido *N*-coordination and two very short metal−pyridine bonds.

(2) For the low-spin iron(III) complex (temperature-dependent magnetic studies) large deviation from octahedral symmetry have allowed us to observe EPR signals even at 298 K.

(3) ^{1}H NMR spectral features of **2** in CD_3CN reveal that its solid-state structure is retained in solution. The observed coordination-induced shifts are the consequences of ligand steric requirements.

(4) Redox properties of **1** and **2** unravel the attainment of a highly stabilized metal(III) state. Interestingly, complex **1**

(17) Drago, R. S. In *Physical Methods in Chemistry*; Saunders: Philadelphia, 1977; Chapter XIII, pp 492−493.
(18) Martin, L. L.; Martin, R. L.; Murray, K. S.; Sargeson, A. M. *Inorg. Chem.* **1990**, *29*, 1387.
(19) (a) Mahapatra S.; Mukherjee, R. N. *J. Chem. Soc., Dalton Trans.* **1992**, 2337 and references therein. (b) Karlin, K. D.; Nasir, M. S.; Cohen, B. I.; Cruse, R. W.; Kaderli, S.; Zuberbühler, A. D. *J. Am. Chem. Soc.* **1994**, *116*, 1324.
(20) A DMF solution of Na_2L at a glassy carbon electrode is electrochemically inactive in the potential range −1.5 to 0.8 V vs SCE. Dark blue solutions of the Fe(II) species in DMF (synthetic reaction) display the expected oxidative response at −0.91 V.
(21) Sigel, H.; Martin, R. B. *Chem. Rev.* **1982**, *82*, 385.
(22) (a) Sawyer, D. T.; Roberts, J. L., Jr. *Experimental Electrochemistry for Chemists*; Wiley: New York, 1974; pp 186, 204−207. (b) Gritzner, G. *J. Phys. Chem.* **1986**, *90*, 5478. (c) Mascharak, P. K. *Inorg. Chem.* **1986**, *25*, 245.
(23) Coulometric oxidation of **1** at 1.3 V reveals that it is a one-electron redox process. The oxidized solution exhibits a cyclic voltammogram similar to Figure S7. However, as expected, now both the responses are reductive.

exhibits solvent-dependent Fe(III)−Fe(II) process. For both complexes a ligand-centered oxidation process is also observed. The exact nature of $1e^-$-oxidized species of **1** is under investigation.

Acknowledgment. This work is supported by grants from the Council of Scientific & Industrial Research (CSIR) and Department of Science and Technology (DST), Government of India, New Delhi. D. G. gratefully acknowledges the award of a fellowship (SRF) by CSIR. The financial assistance of the National X-ray diffractometer facility by DST at this Department is gratefully acknowledged. We thank Dr. B. K. Roy and Mr. A. K. Patra for technical assistance.

Supporting Information Available: Listings of crystallographic experimental details, positional and isotropic thermal parameters, bond distances and angles, dihedral angles, anisotropic thermal parameters, least-squares planes, and hydrogen atom coordinates for compounds **1** and **2** (Tables S1−S16), magnetic data for **1** (Table S17), X-ray structure of **2** (Figure S1), UV−vis spectra of **1** and **2** (Figure S2), EPR spectra of **1** (Figures S3 and S4), ^{1}H NMR spectra of H_2L (Figure S5) and **2** (Figure S6), cyclic voltammograms of **1** and **2** (Figures S7 and S8), and least-squares plot of $E_{1/2}$ (Fe(III)-Fe(II)) of **1** vs reciprocal of dielectric constant of the solvents (Figure S9) (36 pages). Ordering information is given on any current masthead page.

IC961118C

Additions and Corrections

1997, Volume 36

Zhengui Yao and Kenneth J. Klabunde*: The Strong Acidity and the Process for Deprotonation of (η^6-Toluene)-$Fe(H)_2(SiCl_3)_2$.

Pages 6A, 2122, and 2123 (Issue No. 10). There is an error in the drawing of 2,2′-bipyridine in the synopsis, Figure 6, and Scheme 4. A bond is missing, making the structure appear to be a naphthalene derivative rather than 2,2′-bipyridine. The structure should be represented as

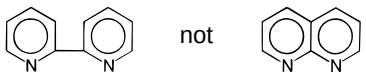

IC970675B

S0020-1669(97)00675-7